Proceedings Paper:
Dawson, J. F. orcid.org/0000-0003-4537-9977, Flintoft, I. D. orcid.org/0000-0003-3153-8447, Duffy, A. P. et al. (2 more authors) (2014) Effect of high temperature ageing on electromagnetic emissions from a PIC microcontroller. In: Electromagnetic Compatibility (EMC Europe), 2014 International Symposium on. 2014 International Symposium on Electromagnetic Compatibility, EMC Europe 2014, 01-04 Sep 2014 IEEE , GBR , pp. 1139-1143.

https://doi.org/10.1109/EMCEurope.2014.6931074

Effect of High Temperature Ageing on Electromagnetic Emissions from a PIC Microcontroller

J F Dawson[1], I D Flintoft[1], A P Duffy[2], A C Marvin[1], M P Robinson[1]
[1] Department of Electronics, University of York, York, UK
[2] Department of Engineering, De Montfort University, Leicester, UK

***Abstract*— This paper describes the effect of high temperature ageing on the electromagnetic emissions of a number of PIC microcontrollers. The aged devices show a measureable shift in the frequency of emissions. Shift in the voltage-current characteristics of the device output pins has also been observed.**

***Index Terms*—radiated emissions, ageing, microcontroller**

I. Introduction

It is an interesting possibility that the ageing of an electronic system might be measured by observing changes in its electromagnetic emissions. This is possibly simpler and less intrusive than waveform monitoring techniques such as suggested in [1]. In particular waveform monitoring is likely to require a number of built in test ports or a means of access to probe internal connections. Emissions monitoring has the potential to observe, simultaneously, many different sources of emissions without making electrical contact with a system.

The effect of ageing on emissions of electronic systems has been observed by a number of authors such as Montanari et al, who examined conducted emissions of computer power supply units [2] and Boyer et al who looked at changes in IC conducted emissions [3]. Here we show how ageing affects the emissions of a Microchip PIC 18F14K22 microcontroller. 17 devices were tested of which 8 were subject to a 1-week ageing process at an ambient temperature of 140 °C. Measurements of the electromagnetic emissions and the voltage current characteristics of output pins were made before and after the ageing process.

II. The PIC Microcontroller System

The PIC microcontroller was chosen as it is one of the few simple devices which can be socket mounted. This allows devices to be aged separately from the remainder of the circuit and also allows different devices to be tested in a single test board, thus ensuring any change of behaviour seen is due to the changes in the microcontroller rather than other circuit elements.

The work presented in this paper has been funded by the EPSRC Centre for Innovative Manufacturing in Through-life Engineering Services under grant EP/1033246/1 project CP15.

A. Test Circuit

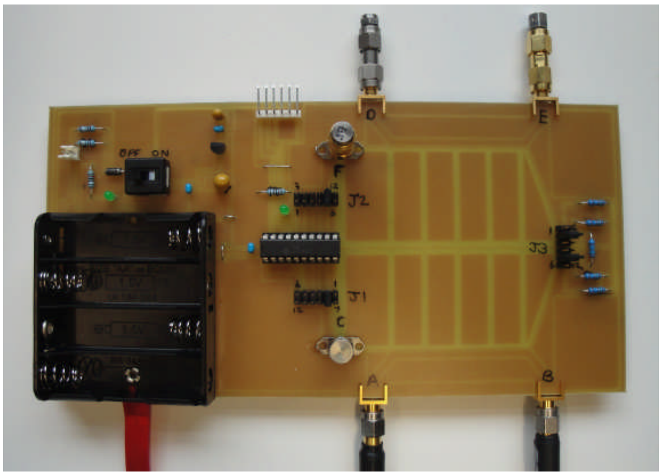

Fig. 1: The microcontroller emissions test circuit board.

The emission test board is shown in Fig, 1.The PIC is powered by 4 rechargeable AA cells via a linear regulator to remove the effect and variability due to external supply connections. LEDs are used to indicate power supply and PIC operation. The latter is flashed slowly on power up to indicate the on-chip software is operational. The PIC device chosen has an on-board clock so no additional components are required for the device to function. A number of Input/Output (I/O) pins are brought to one of two header strips near the PIC which allow them to be connected to one of two loaded tracks which each pass an RF coupler. The track loads can be selected by means of further jumpers on the right hand side of the board (Fig. 1) and schematically in Fig. 2.

B. RF Couplers

In order to ensure good repeatability of the RF emissions measurement, we included RF couplers on the circuit board. These can be seen in Fig. 1 on the right hand side of the board at the top and bottom.

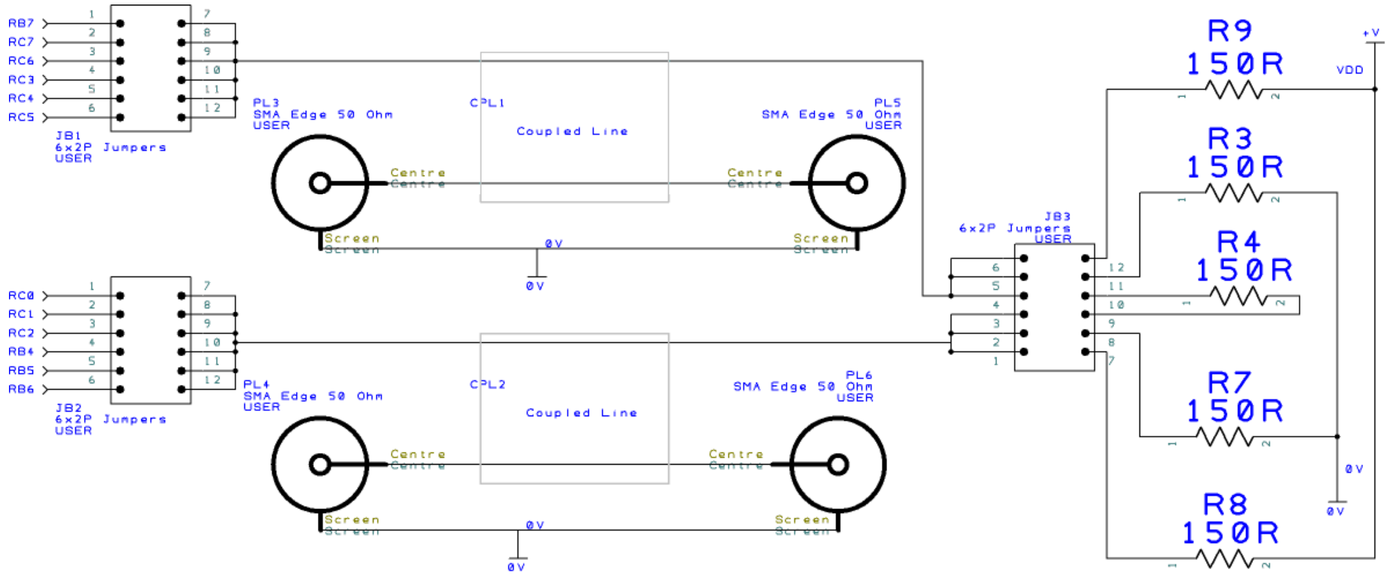

Fig. 2: PIC input/output pin connections via jumper banks and RF couplers to load selection jumpers.

An edge mounted SMA connector is provided at each end of the coupler. The couplers are also shown schematically in Fig. 2. Fig. 3 shows the detailed board layout. The coupler is designed to have a 50 Ω impedance to give a good match as the SMA connectors. An SMA connector is also attached at the PIC end of the IO track, near the PIC so the coupler can be characterised. The ground plane sections near the I/O tracks are broken to maximise the coupling to the coupler track.

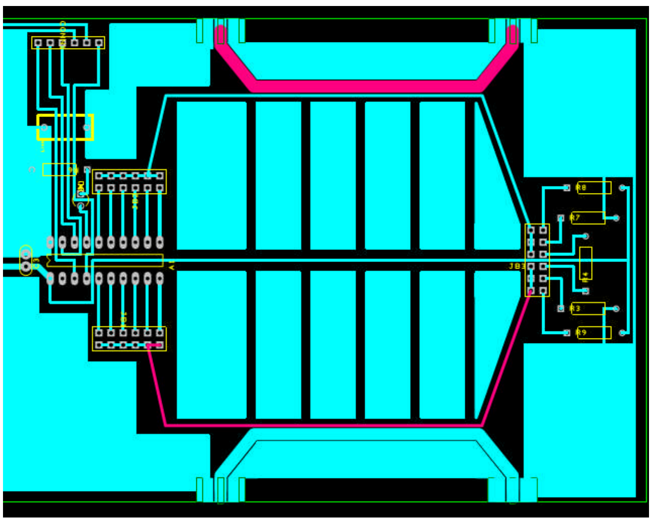
Fig. 3: Layout of the underside of the circuit board showing the RF couplers.

Fig. 4 shows the S-parameters of one of the couplers. Ports A (near PIC) and B (near loads) are the edge mounted SMA connectors and port C is the IO track near the PIC. The coupler has a through (A to B) loss of less than 3 dB up to 1 GHz and less than 6dB up to 6 GHz. The coupling to port C is directive and increases smoothly with frequency up to 100 MHz after which some resonant behaviour is observed as the I/O track termination resistors are not an accurate match and the physical layout adds significant inductance..

For emissions measurements the ports nearest the PIC were used (for maximum coupling to the PIC) with the other end of the coupler terminated with a 50 Ω load. The I/O track is loaded only by the PIC and a 150 Ω resistor to ground, the vertically mounted SMA connector being left open.

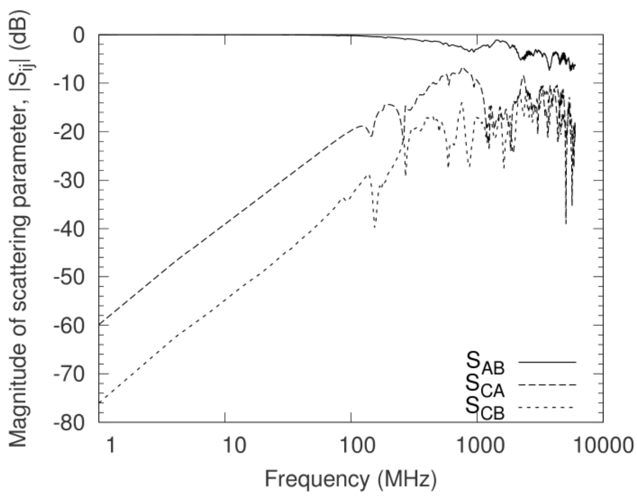

Fig. 4: Coupler performance.

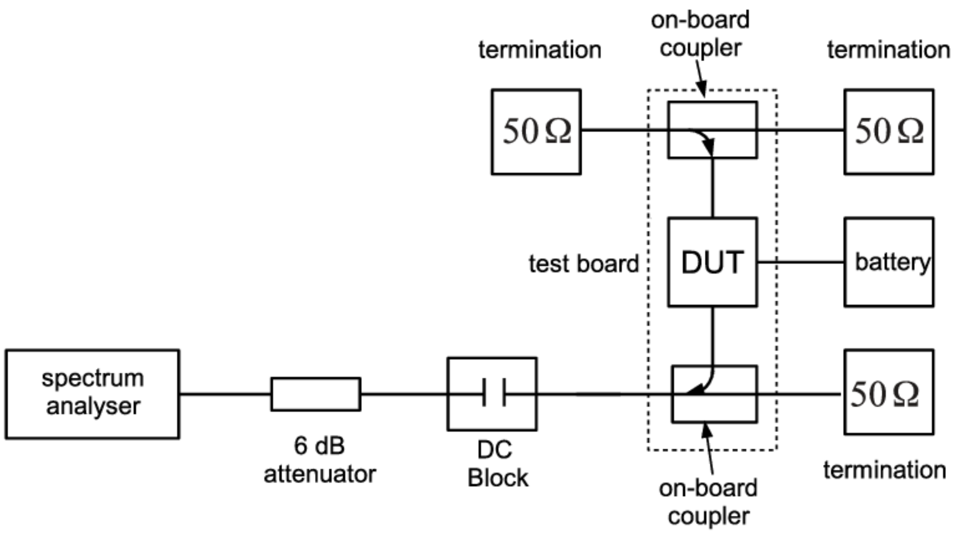

Fig. 5: The measurement system.

C. *Software*

The software used for test purposes, after checking the presence of, and flashing the LED on port A, setting the device to operate as the maximum clock frequency of 64 MHz, and configuring port C as outputs, toggles alternate I/O pins on port-C of the PIC as fast as possible to maximize interference generation.

If the LED (pull down) is not detected the software enters an alternate state used for I/O pin measurements where the port C outputs can be manually toggled using a push button with a pull-up resistor connected to the same pin.

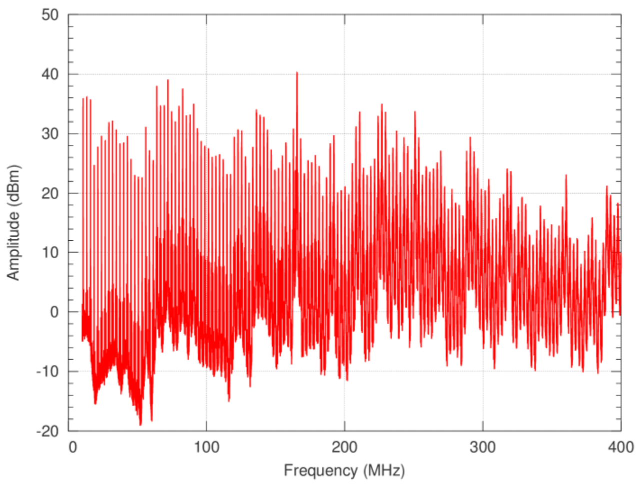

Fig. 6: The full emissions spectrum of PIC M01 from 10 MHz to 400 MHz before ageing.

I. Ageing the Microcontroller

Eight of the microcontrollers were aged for one week at 140°C in a thermally controlled oven. During the ageing process the microcontrollers were powered with the emissions software running but with only the indicator LED connected to port A.

I. Emissions Measurement

Fig. 5 shows the measurement set-up. In order to prevent damage to the spectrum analyser an attenuator and DC block is used. All unused coupler ports were terminated with 50 Ω loads. The emissions spectrum was measured from each device over the range 10 MHz to 400 MHz. This was the range over which emissions of a significant amplitude occurred whilst allowing enough measurement points to be achieved in a single sweep to be able to observe detail in the region of each harmonic.

II. Emissions Results

Fig. 6 shows the full emissions spectrum from SMA port A, connected to IO port C pin 7 of PIC M01. As expected the spectrum consists principally of harmonics of about 2.6 MHz – the frequency at which the IO lines are toggled.

Fig. 7 shows detail around the 27 MHz harmonic before and after ageing. It can be seen that the harmonic has sidebands at about ±500 kHz. The harmonic and sidebands both shift in frequency due to the ageing process. Fig. 8 shows the detail around 99MHz where a larger shift in the harmonics can be seen due to ageing.

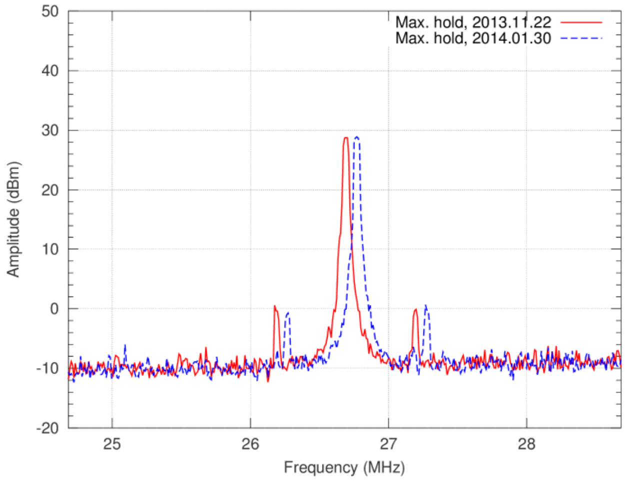

Fig. 7: Shift in the emission spectrum of PIC M01 about an harmonic at 27 MHz due to ageing for 1 week at 140°C. (aged = dashed line)

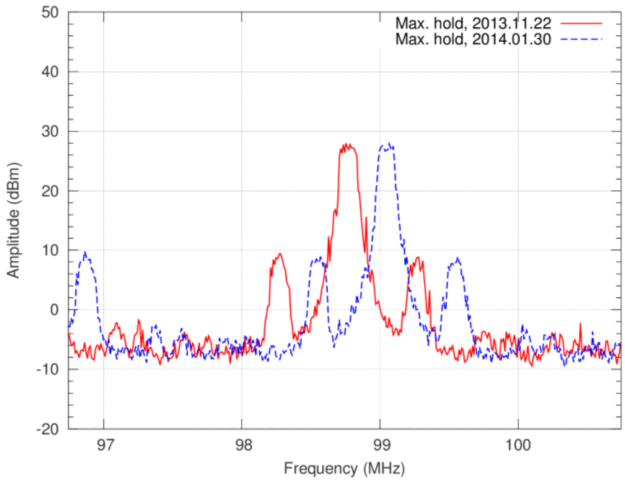

Fig. 8: Shift in the emission spectrum of PIC M01 about an harmonic at 99 MHz due to ageing for 1 week at 140°C (aged = dashed line).

Fig. 9 and Fig. 10 show the same measurements for PIC M09 taken at the same time. PIC M09 was not aged and the measurements show good repeatability.

The amplitude and frequency of the harmonics around 27 MHz and 99 MHz were extracted from the data and are presented in Fig. 11 and Fig. 12. PICs M01-M08 were subject to the one week ageing period and PICs M09-M13 were not aged. PIC M14 was used for a short, 3 day, ageing test.

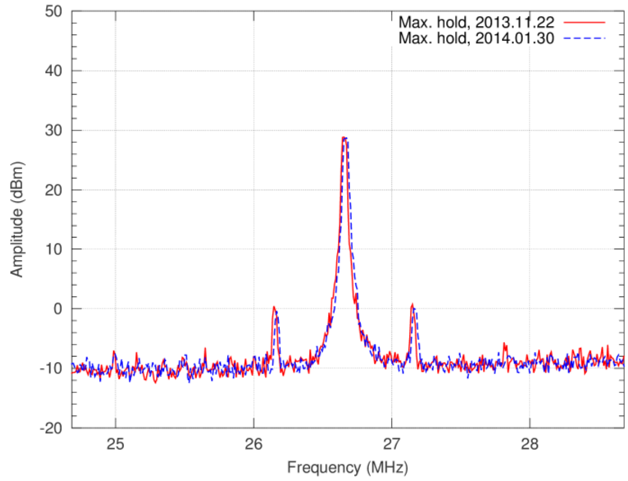

Fig. 9: Repeatability of the emission spectrum measurement of PIC M09 for the harmonic near 27 MHz for an unaged device.

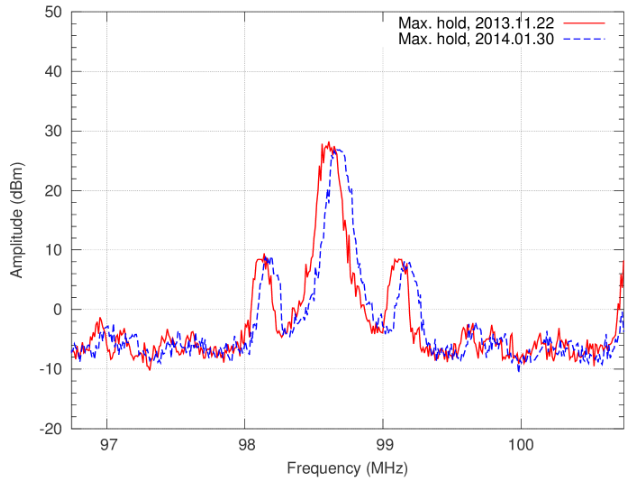

Fig. 10: Repeatability of the emission spectrum measurement of PIC M09 for the harmonic near 99 MHz for an unaged device.

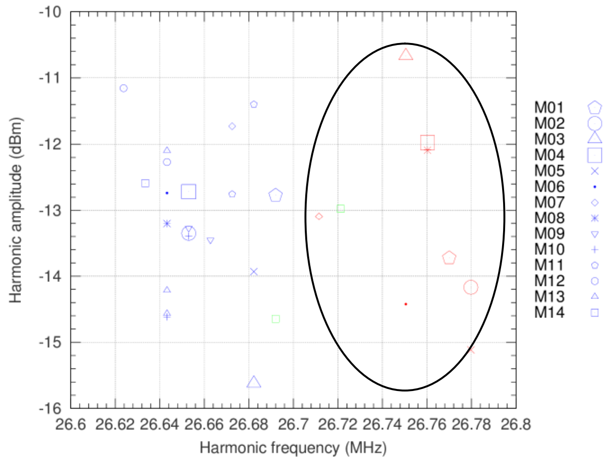

Fig. 11: Change in amplitude and frequency of an emissions harmonic peak near 27 MHz for 14 PICs. Blue is unaged, green aged for 3 days and red aged for 1 week (aged circled).

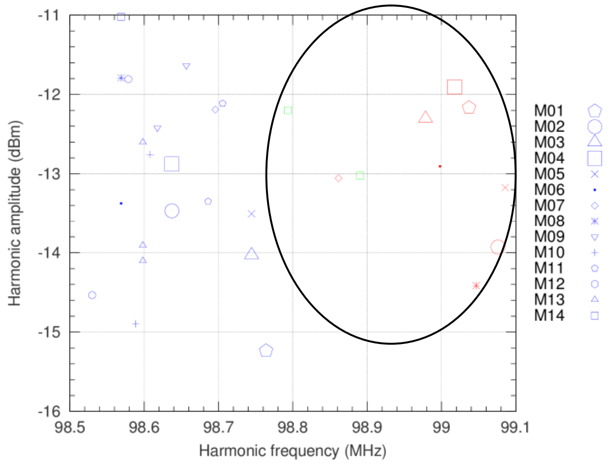

Fig. 12: Change in amplitude and frequency of an emissions harmonic peak near 99 MHz for 14 PICs. Blue is unaged, green aged for 3 days and red aged for 1 week (aged circled).

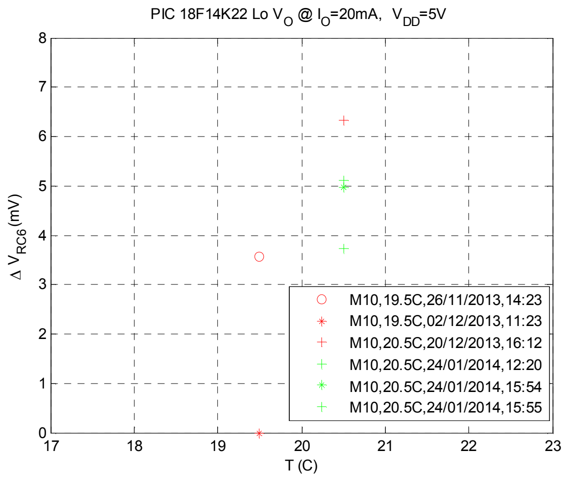

Fig. 13: Change in PIC M10 Port C pin 6 Low output voltage as a function of temperature and different measurement dates (no ageing).

I. IO PIN CHARACTERISTICS

The voltage/current curves were measured for port C pins 6 and 0 for each of the devices, before and after ageing. Fig. 13 shows a number of measurements of the low output voltage at a current of 20 mA for PIC M10, taken on different dates at different temperatures. It can be seen that the voltage measured varies from measurement to measurement and tends to be higher at the higher temperature. The overall variation from lowest to highest measurement is just over 6 mV. This is typical of the set of devices.

Fig. 14 compares a number of measurements for PIC M06 before and after ageing. It can be seen that the post ageing measurements show an increase in output voltage of about 10mV over those measured prior to ageing.

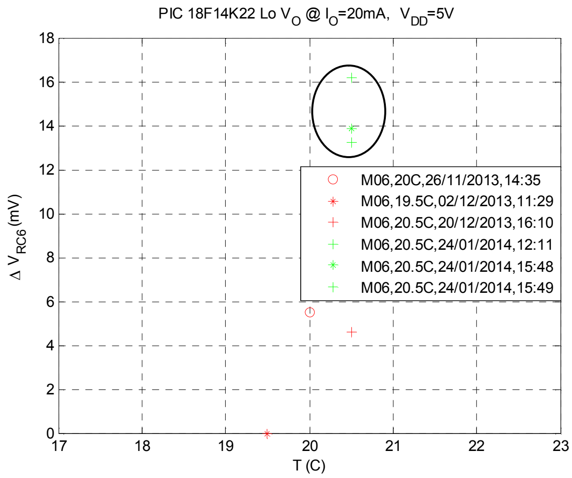

Fig. 14: Change in PIC M06 Port C pin 6 Low output voltage as a function of temperature and different measurement dates, before (2013 dates) and after ageing (24/01/2014) (aged circled).

II. CONCLUSIONS

We have shown that high temperature ageing of a PIC device results in a measureable change in the frequency of electromagnetic emissions that might be used as an indicator of ageing. The change in emissions was accompanied by a change in the voltage/current characteristics of the output ports. Having seen the amplitude of the re-emissions spectra of some electronic systems change when exposed to differing levels of interference [4], we had hoped also to see some change in the amplitude of the emissions as the characteristics of the devices changed with ageing. Work is currently being carried out to age further the devices in order to see how these changes develop as the devices degrade.

Unfortunately, in this study we have not had the resource to investigate in detail the reasons for the changes observed. However it seems likely that the ability to detect such changes offers the potential to detect ageing and incipient failure in a range of electronic systems.

REFERENCES

[1] B. Saha, J. Celaya, P. Wysocki and K. Goebel, "Towards prognostics for electronics components,", *IEEE Aerospace Conference 2009*, Big Sky, MT, pp. 1-7, 7-14 Mar., 2009.

[2] I. Montanari, A. Tacchini and M. Maini, "Impact of thermal stress on the characteristics of conducted emissions," *IEEE International Symposium on Electromagnetic Compatibility 2008, EMC 2008*, Detroit, MI, pp. 1-4, 18-22 Aug., 2008.

[3] A. Boyer, S. Ben Dhia, B. Li, N. Berbel and R. Fernandez-Garcia, "Experimental investigations into the effects of electrical stress on electromagnetic emission from integrated circuits," *IEEE Transactions on Electromagnetic Compatibility,* vol. 56, no. 1 , pp. 44-50, 2014.

[4] I. D. Flintoft, A. C. Marvin, M. P. Robinson, K. Fischer and A. J. Rowell, "The re-emission spectrum of digital hardware subjected to EMI," *IEEE Transactions on Electromagnetic Compatibility,* vol. 45, no. 4 , pp. 576-585, 2003.